Insights into the catalytic mechanism of type VI sulfide: quinone oxidoreductases

Ágnes Duzs [a,b,1], Nikolett Miklovics [a,b,c,1], Gábor Paragi [d,e], Gábor Rákhely [a,b,*,1], András Tóth [a,b,1]

[a] Institute of Biophysics, Biological Research Centre, Temesvári krt 62., H-6726 Szeged, Hungary
[b] Department of Biotechnology, University of Szeged, Közép fasor 52., H-6726 Szeged, Hungary
[c] Doctoral School in Biology, University of Szeged, Közép fasor 52., H-6726 Szeged, Hungary
[d] Institute of Physics, University of Pécs, Ifjúság útja 6., H-7624 Pécs, Hungary
[e] MTA-SZTE Biomimetic Systems Research Group, Department of Medical Chemistry, University of Szeged, Dóm square 8, H-6720 Szeged, Hungary

ARTICLE INFO

ABSTRACT

Sulfide oxidation is catalyzed by ancient membrane-bound sulfide:quinone oxidoreductases (SQR) which are classified into six different types. For catalysis of sulfide oxidation, all SQRs require FAD cofactor and a redox-active centre in the active site, usually formed between conserved essential cysteines. SQRs of different types have variation in the number and position of cysteines, highlighting the potential for diverse catalytic mechanisms. The photosynthetic purple sulfur bacterium, *Thiocapsa roseopersicina* contains a type VI SQR enzyme (TrSqrF) having unusual catalytic parameters and four cysteines likely involved in the catalysis. Site-directed mutagenesis was applied to identify the role of cysteines in the catalytic process of TrSqrF. Based on biochemical and kinetic characterization of these TrSqrF variants, Cys121 is identified as crucial for enzyme activity. The cofactor is covalently bound via a heterodisulfide bridge between Cys121 and the C8M group of FAD. Mutation of another cysteine present in all SQRs (Cys332) causes remarkably decreased enzyme activity (14.6% of wild type enzyme) proving important, but non-essential role of this residue in enzyme catalysis. The sulfhydril-blocking agent, iodoacetamide can irreversibly inactivate TrSqrF but only if substrates are present and the enzyme is actively catalyzing its reaction. When the enzyme is inhibited by iodoacetamide, the FAD cofactor is released. The inhibition studies support a mechanism that entails opening and reforming of the heterodisulfide bridge during the catalytic cycle of TrSqrF. Our study thus reports the first detailed structure-function analysis of a type VI SQR enzyme which enables the proposal of a distinct mechanism of sulfide oxidation for this class.

1. Introduction

Sulfur is one of the most crucial elements for living organisms. Its most reduced and reactive form, sulfide (H_2S. HS^-, S^{2-}) is toxic to cells primarily due to inhibition of hemoproteins involved in electron transport chains (e.g., cytochrome *c* oxidase) [1–3]. Despite its toxicity, sulfide is an essential metabolite during the biosynthesis and catabolism of important sulfur-containing cellular compounds, such as methionine, cysteine and iron-sulfur clusters [4]. Besides, it can also be an energy and electron donor for microorganisms living in sulfide-rich environments [5,6]. In eukaryotes, sulfide and its derivatives are recognized as cell modulators and signal molecules, participating in diverse physiological processes, similarly to the other gasotransmitter compounds, such as nitric oxide (NO) and carbon monoxide (CO) [7–9]. Inappropriate control of sulfide concentration is associated with various pathological processes, such as neurodegenerative diseases, cancer, and diabetes [10,11].

Sulfide:quinone oxidoreductases (SQR) are ancient monotopic membrane-bound flavoproteins, which were essential for the early life forms living in the sulfidic oceans of the primordial Earth [12,13], and now ubiquitous in all organisms except plants [5,6]. SQR enzymes belong to the Flavoprotein Disulfide Reductase (FDR) enzyme family [14] acting on the most reduced form of sulfur (sulfide), thus offering a first crucial step to detoxification. SQRs catalyze the oxidation of sulfide

---

```
Type I     A. ferrooxidans     NPWVGVGWK   SIC-TVDH   -MAGASCF-GPAYE   FVLVDEHQ-   NAVCFADMGD     C        C
           R. capsulatus       NPWVAVGWR   SIC-HIDH   -AQGASCF-GPAYE   FVIVDQHQ-   NAVCLADFGD   C
           A. aeolicus         FPHLAMGWR   SIC-TAEH   -IPGVSCF-GPAYE   MVIVNRCF-   SAICIADFGE
                                           C124        C156                        C347

Type II    H. sapiens          WTLVGAGAK   SNY-SVKT   PNTPVKCA-GAPQK   WVDVDKETL   YTSCPLVTGY     C        C
           Synechocystis sp.   WTLVGGGAF   SNY-DRRY   PATPIKCA-GAPQK   WVDVDKFTL   YTCCPLVTGY
           S. pombe            WTLTGAGLS   TIY-SEKY   PSGVLKCA-GAPQK   FVAVDQSTT   YTSCPLLTGY

Type III   S. solfataricus     QLLVGFGLE   TVY-EYDD   AKLPHRCP-VAPLE   WVPTDKFTL   DVLCYIATGT     C        C
           C. tepidum          LLFVPFGVQ   TFY-YKEA   AELPFKCP-VAPIE   YVPTHHNTL   HSTCFIVYSK
           C. maquilingensis   LLYIAFKGS   YHS-SEEN   SYERYRCP-PSPLE   FVLADNATN   RTHCPFDMGY

Type IV    A. vinosum          NIWVGVGEM   SVC-TPSH   GHGMCTCQ-GAAFE   FMKVDADYN   GAACVASTGM     C        C
           S. denitrificans    NIWVGVGEM   SVC-TADH   GHGLCTCQ-GAAFE   FMKVDANYS   GAACVASAGK   C
           C. tepidum          NIWVGVGHM   SVC-TYSH   GHAMATCQ-GAAFE   FMKVDADYT   GAACIVSAGF

Type V     A. ambivalens       LPHVAIGVR   SVC-EPEF   PNADSACE-GPVFE   FIPTDLNMV   TIMCVADNPY     C        C
           S. solfataricus     LPHVATGVI   SVC-ELDY   PVADAACE-GPIFE   FVPTDLNMV   TIICVADNPF   S/C
           C. tepidum          ILMEILENK   TVS-DGFY   PMAKAACE-GPPVE   FVITNKQLK   EVICYGDMGD

Type VI    C. tepidum          AIWIPVGTE   SICGAPEH   --DPSAVRGGPGFE   FVKIDDFCR   NVLCVMDTGD              C
           A. vinosum          LIWVPSGLR   VPCEGVVA   --EPSSMRGGPVFE   LLQADAHCR   ELLCIVDTND   C
           T. roseopersicina   LIWVPCGIR   TPCEGIAA   --EPSSMRGGPIFE   LLQADAHCR   ELVCIVDAND                 C
                                   C49     C121                          C272      C332
```
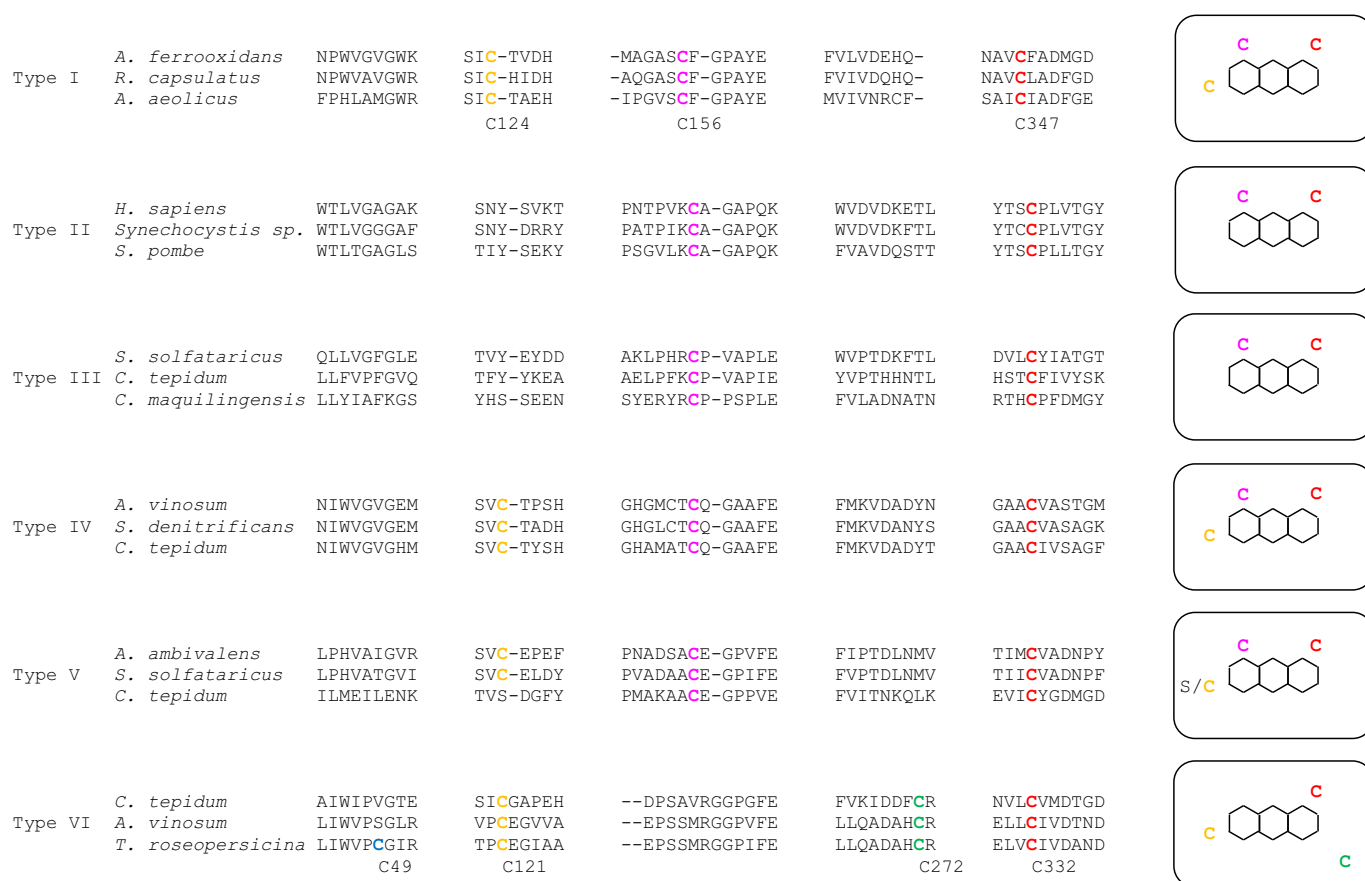
Fig. 1. Multiple sequence alignment of selected representative SQR proteins with conserved cysteines in the primary sequence of various sulfide:quinone oxido-reductases (*Aquifex aeolicus* and *Thiocapsa roseopersicina* residue numbering). The diagrammatic scheme (far right) indicates the approximate location of conserved cysteines in relation to the isoalloxazine ring of FAD, based on the structures of various sulfide:quinone oxidoreductases.

to sulfur via electron transfer to the membrane quinone pool in micro-organisms and mitochondria. In addition to a role in sulfide detoxification, SQRs can be involved in sulfide-dependent bioenergetics and eukaryotic sulfide homeostasis.

SQR proteins have been classified into six types (types I–VI, SqrA–F), each with characteristic sequence motifs and structural elements [12] (Fig. 1). More recently, a thorough bioinformatic analysis of all available SQR sequences has also distinguished six classes and recognized a new group of essentially archaeal SQRs [6]. The later study excludes the previously identified type VI subfamily discounting it as a sulfide: quinone oxidoreductase type based on the required sequence criteria. However, in this study, we follow the classification of Marcia et al. [24].

The biochemical, enzymatic, and structural characterization of SQR enzymes has been limited by the difficulties in their isolation in a stable, active form from their natural host [15,16] or via heterologous protein expression [17–23] in, for example, *E. coli*. The SQR enzymes catalyze a complex redox reaction composed of reductive and oxidative half-reaction. Similarly to all members of FDR enzyme family, for the catalysis, SQR enzymes require Flavine Adenine Dinucleotide (FAD) cofactor and a redox-active disulfide bridge usually formed between the conserved internal cysteines in the active centre of the enzyme [12,22,24–26]. The reductive phase combines the reduction of FAD with the oxidation of sulfide resulting in the formation of cyclooctasulfur rings or polysulfide chains of sulfur atoms. The polymerization of the oxidized sulfide substrate molecules requires the contribution of the redox-active disulfide bridge. The second oxidative half reaction is simpler, in which electrons are transferred from the reduced FAD to the electron acceptor; a quinone compound in the membrane [27].

Primary sequence comparison of SQRs reveals the presence of

cysteine residues in the proteins, conserved at various levels across the various types [12]. Furthermore, site-directed mutagenesis studies have indicated their importance in the catalytic activity of these enzymes. Cysteines, corresponding to the Cys347 residue of *Aquifex aeolicus* type I SQR, are present in all known SQR proteins and also cysteines corresponding to Cys156, except for type VI enzymes (Fig. 1). Single point mutations of these cysteines to serine or alanine in the type I SQR of *Rhodobacter capsulatus* and *Acidithiobacillus ferrooxidans* resulted in drastically reduced activity and/or inactive proteins [17,18], indicating their essential role in the catalytic function of SQR enzymes. A third cysteine, Cys124, is also highly conserved, but is absent in type II, type III and few type V SQR proteins. Its essential role in type I SQRs is highlighted by the drop of activity to approximately 1% of the wild-type enzyme upon its replacement by serine [17]. Interestingly, type VI SQR proteins have a slightly different set of conserved cysteines across all known representatives that therefore appear to be characteristic of this set. This difference will be discussed further later.

So far, the crystallographic structures of two type I SQRs [18,24,26], one type II SQR [22] and a type V SQR [25] have been determined. Based on the known SQR crystallographic structures, the conserved cysteines are located in the active centre of the enzymes near to the isoalloxazine ring of FAD cofactor. The relative position of the conserved cysteines in the various SQR proteins is schematically represented on the right-side panel of Fig. 1. The SQR structures (for the group I, II and V SQRs) revealed that a redox-active disulfide-bridge is formed by two conserved cysteines close to FAD located at the active site, which contain the residues corresponding to Cys156 and Cys347 of *A. aeolicus* SQR [22,24–26].

The FAD cofactor is bound either covalently or non-covalently to the

active site of the protein. A covalent bond is formed between the thiol group of homologues of the Cys124 residue of *A. aeolicus* and the C8M methyl group of the isoalloxazine moiety. Crystal structures show that in the type V SqrE enzyme of *Acidianus ambivalens*, a stable thioether bond is formed [25], but in the type I SqrA enzyme of *A. aeolicus,* a putative persulfide bond provides the link between the protein and the cofactor [24]. The FAD is bound non-covalently in the type I *A. ferrooxidans* and *R. capsulatus* SqrAs [17,26], the type II human SQR [22] and the type III SqrC of the hyperthermophilic archaeon, *Caldivirga maquilingensis* [19].

The mechanisms of the SQR-catalyzed reactions are poorly understood. The aforementioned variations of the conserved cysteine patterns (see Fig. 1) and the chemical nature of FAD-binding indicate that there may also be differences in their catalytic mechanisms. The proposed requirement of the disulfide bridge formed between two conserved cysteines during the reductive phase has some support from structural and biochemical studies. It is suggested that the dissociated H_2S (SH^-) initially reacts with the disulfide bridge formed by cysteines (between Cys156 and Cys347 in the *A. aeolicus* SqrA) through a nucleophilic attack mechanism. This reaction breaks up the disulfide bond generating a reduced thiolate form of one cysteine and promotes the formation of the intermediate charge-transfer complex between the other cysteine and the isoalloxazine ring of FAD. In the case of the "C4A mechanism", the charge transfer complex uses the C4A carbon of the FAD isoalloxazine ring either directly or by the incorporation of an additional sulfur (partially oxidized sulfide substrate) into the protein-FAD complex [17,18,22,24–26,28]. In an alternative model, the "C8M mechanism" described for the *A. aeolicus* SqrA enzyme, the redox-active disulfide bridge is formed between Cys124 and Cys156, and the consequent charge transfer complex involves Cys124 and the C8M group of the isoalloxazine moiety of FAD [24]. After the oxidation of FAD, a transient $Cys124\text{-}S\text{-}S^+$ is formed which reacts with the $Cys156\text{-}S^-$ yielding a trisulfide bridge. The Cys347 takes over the growing sulfur chain, thus regenerating $Cys156\text{-}S^-$ for the next cycle. The catalytic cycle repeats multiple times, forming a ring or linear chain of sulfur (octasulfur ring or polysulfide) [12].

Thiocapsa roseopersicina, a model organism of photosynthetic purple sulfur bacteria, utilizes various reduced inorganic sulfur compounds (e. g. sulfide, sulfur, thiosulfate, sulfite) as electron and energy sources for its anoxygenic photochemolioautotrophic growth [29,30]. The bacterium has complex sulfur metabolism for the oxidizing and/or reducing sulfurs of various oxidation states [31,32]. In the genomic sequence of *T. roseopersicina* [33], genes of two SQR enzymes of types IV and VI SQRs, SqrD and SqrF, respectively, were discovered [16]. The genes coding for another sulfide oxidase enzyme complex, flavocytochrome c sulfide dehydrogenase (Fcc), were also identified which interestingly has a sulfide-oxidizing subunit homologous to SQR enzymes (Balogh et al., personal communication) [16]. In the TrSqrF protein, there are four cysteine residues, which are likely involved in the catalytic cycle.

Previous biochemical analysis of homologously-expressed and purified recombinant TrSqrF enzyme demonstrated that the protein contains a covalently bound FAD cofactor [16], in common with some other SQRs. The kinetic parameters of the enzyme, however, are different from those of any other characterized SQRs [16]. The catalytic mechanism of type VI sulfide:quinone oxidoreductases has not been characterized yet.

In the study presented here, we perform a functional investigation of TrSqrF cysteine residues and propose a novel mechanistic model for catalysis of type VI sulfide:quinone oxidoreductases.

2. Materials and methods

2.1. Bacterial strains, plasmids, primers and nucleotide sequences

Bacterial strains [16,34], plasmids [16,35,36] and PCR primers used are listed in Tables S1, S2 and S3, respectively. Nucleotide sequence data are available in the GenBank database under the accession numbers KY595104 (*sqrD*), KY595105 (*sqrF*), KY595103 (*fccAB*).

2.2. Growth conditions

E. coli and *T. roseopersicina* cells were grown as described in Duzs et al. [16].

In brief, *E. coli* cells were grown in Luria-Bertani Broth medium with 25 μg/mL kanamycin or 100 μg/mL ampicillin. *T. roseopersicina* strains were grown photoautotrophically in modified Pfennig's medium containing 4 g/L sodium thiosulfate [37] supplemented with genotype-specific antibiotics (streptomycin: 25 μg/mL, gentamycin: 25 μg/mL, kanamycin: 25 μg/mL) under anaerobic conditions. The *T. roseopersicina* cultures were incubated at 25 °C for 4 days under illumination.

2.3. Construction of fcc, sqrD and sqrF deletion mutant T. roseopersicina strain

In order to delete the *sqrD* gene, the upstream region of the *sqrD* gene was amplified with the osqr1F–osqr2R primer pair using a Phusion polymerase. The amplicon was treated with kinase and ligated into an *Eco*RV-digested Bluescript vector (creating pSQRUP). The *sqrD* upstream fragment was cleaved with *Eco*RI and *Bam*HI from the pSQRUP and inserted into *Eco*RI-*Bam*HI-digested pK18mobsacB (pKSQRUP). The downstream region of *sqrD* gene was amplified with the osqr3F-osqr4R primers and inserted into an *Eco*RV-digested Bluescript vector (pSQRDO). The pSQRDO and the pKSQRUP vectors were cleaved by *Xba*I-*Hind*III and the *sqrD* downstream region was ligated into the *Xba*I-*Hind*III digested pKSQRUP vector (pKDSQR). The pKDSQR plasmid was transformed into a conjugation-helper *E. coli* S17-1 λpir strain, then conjugated [38] into *T. roseopersicina* FOX (see Table S1) cells (FOQR). The construction of the *sqrF* gene deletion was carried out as described in Duzs et al. [16], and the pKDSQN was conjugated into *T. roseopersicina* FOQR cells resulting in the FOQRON strain.

2.4. Construction of vectors expressing TrSqrF mutants

In order to construct the mutant TrSqrF-expression vectors, the wild type *TrsqrF* gene in pBNSQNNS [16] plasmid was used as a template for site-directed mutagenesis. The reaction mix contained 20 ng template, 200 μM dNTP, 10× Phusion HF buffer and 125–125 ng of the mutagenesis primer pairs (onC121AF-onC121AR; onC272AF-onC272AR; onC332AF-onC332AR; onC49AF-onC49AR) in 50 μL total volume. DNA amplification with these primers was initiated by the addition of 2.5 U Phusion DNA polymerase. The applied program was as follows: 1× (30 s at 95 °C), 16 times: (30 s at 95 °C, 1 min at 55 °C), then 1× (6 min at 72 °C). *Dpn*I (10 U/μL) was added into the reaction and incubated at 37 °C for 1 h; then the reaction mix was transformed into XL1-Blue MRF′ cells. Selected clones were sequenced to confirm the successful mutation of the *sqrF* gene. Vectors containing the mutant *sqrF* fragments (pBNSQNNSC121A; pBNSQNNSC272A; pBNSQNNSC332A; pBNSQNNSC49A) were cleaved by *Hind*III, the ends were polished by Klenow enzyme and cleaved by *Nde*I endonuclease. The pDSK6CrtKm expression vector was digested by *Pst*I, blunted using T4 DNA polymerase and cleaved by *Nde*I; then the mutant *sqrF* fragments were inserted into this vector (pDSQNNSC121A; pDSQNNSC272A; pDSQNNSC332A; pDSQNNSC49A). The expression vectors were conjugated (Fodor et al. 2001) into the *T. roseopersicina* FOQRON strain via the appropriate *E. coli* S17-1 lambda pir cell line, resulting in the strains named according to mutation: TrC121A; TrC272A; TrC332A; TrC49A, respectively (see also Tables S1 and S2).

2.5. Expression and purification of TrSqrF protein variants

T. roseopersicina cultures expressing TrSqrF mutants were grown in modified Pfennig's medium in 2 L flasks at 25 °C for 4 days. Cells were centrifuged at 8300 ×*g* at 4 °C for 10 min. In order to eliminate the

periplasmic cell fractions, harvested cells were suspended in the periplasmic buffer (150 mM NaCl, 50 mM Tris pH = 8.0, 25% sucrose and 0.1% lysozyme) and incubated at 30 °C for 30 min. An equal volume of cold distilled water was added, and the cells were incubated on ice for 10 min. After centrifugation (13,700 $\times g$; 4 °C, 10 min), the periplasmic fractions were discarded, the spheroplasts were suspended in TBS buffer (150 mM NaCl, 50 mM Tris pH = 8.0). To disrupt the spheroplasts, the suspensions were sonicated for 15 s 8 times applying 7 kJ energy on ice (Bandelin Sonoplus HD3100) and centrifuged (27,000 $\times g$, 4 °C, 15 min).

The resulting crude cell extracts were ultra-centrifuged (Sorwall WX Ultra Series) (100,000 $\times g$, 4 °C, 90 min), and the pellet (membrane fraction) was suspended in TBS buffer. The membrane fractions were treated with 10 mM EDTA (pH =8.0) for 30 min at 25 °C, followed by addition of 1.45 M sodium-bromide and were further incubated at 25 °C for 60 min. The treated membrane fractions were ultra-centrifuged (200,000 $\times g$, 4 °C, 120 min), and the supernatant containing the TrSqrF variants were stored at −20 °C. Recombinant, mutant TrSqrF proteins were purified via StrepII tag using Strep-Tactin Superflow high capacity resin at room temperature based on the instructions of the manufacturer (IBA Lifesciences, Cat. No.: 2-1208-002).

2.6. Protein analytical methods

The purified TrSqrF mutants were analyzed on 12% SDS-polyacrylamide gels [39]. Protein (1 μg of protein/sample) was loaded onto denaturing gels, and the bands were visualised by Blue Silver dye [40]. For western blotting, Strep-Tag II specific monoclonal antibody (IBA Lifesciences) was applied, and chemiluminescent detection was carried out using the SuperSignal West Pico Rabbit IgG Detection Kit (Thermo Scientific). The TrSqrF protein bands and signals were recorded by the VersaDoc 4000MP gel-imaging system (BIO-RAD). For determination of the molecular weight of the purified proteins, Prosieve Quadcolor Protein Marker was used (cat. no.: 00193837). The concentrations of purified TrSqrF protein variants were determined using the Lowry method [41].

2.7. Spectroscopic assays

The UV–visible absorption spectra of the purified proteins were obtained by placing samples in a quartz cuvette and recording the absorbance over a wavelength range of 300–600 nm using a spectrophotometer (Nicolet Evolution 300, Thermo Scientific). Absorption spectra of the TrSqrF mutants of various concentrations were normalized so, that the maximum absorbance values of the spectra were the same.

2.8. Enzyme activity assay

Sulfide-dependent quinone reduction activity of the TrSqrF variants was measured in Suba-seal septa (Sigma-Aldrich) sealed, nitrogen-flushed quartz cuvettes under anaerobic conditions. For standard activity measurements, 50 mM Tris-HCl buffer, pH = 8.0, 50 μM duroquinone and 3.3 μg purified enzyme were combined in a 1 mL final volume. The reduction of duroquinone (molar extinction coefficient at 275 nm: 16 mM^{-1} cm^{-1}) [42] was recorded at 275 nm at 25 °C using a spectrophotometer (Nicolet Evolution 300, Thermo Scientific) immediately after addition of 200 μM anaerobically and freshly prepared sulfide to the reaction mix. The kinetic constants were determined using various concentrations of duroquinone (10–100 μM). The sulfide dependence of the mutant TrSqrF activities was measured in the 50–750 μM concentration range. The data were curve-fitted by non-linear regression analysis of MatLab software [43]. One unit of sulfide:quinone oxidoreductase activity was defined as the amount of enzyme that achieves the reduction of 1 μmol duroquinone per min. At least three independent experiments were performed and evaluated.

2.9. Enzyme inhibition assay

Inhibition of TrSqrF enzyme activity by iodoacetamide was performed as a standard activity measurement in the presence of sulfide and duroquinone and using 25–250 μM iodoacetamide. To study the connection between the inhibition of enzyme activity and flavin binding, 25 μM TrSqrF was mixed with 50 μM duroquinone and 200 μM sulfide in the presence or absence of 500 μM iodoacetamide and incubated at room temperature for 10 min. Samples were taken for activity measurement from the mixtures, and the remaining reaction mixes were diluted 10 times to record the UV–visible absorption spectrum of the treated TrSqrF. The enzyme was precipitated with 5% trichloroacetic acid and centrifuged (4500 $\times g$, 4 °C, 15 min,) [44]. The absorption spectra of the supernatants and the pellets suspended in 0.25 mM NaOH were recorded by a spectrophotometer (Nicolet Evolution 300, Thermo Scientific). To determine the presence of unbound FAD, the suspended pellets were filtered through a 10 kDa Amicon Ultra centrifugal filter (Millipore) and the absorption spectra of filtrates documented.

2.10. TrSqrF homology model

For homology building, the Prime [45,46] module of the Schrodinger [47] suit was applied. Templates for homology modelling were found by a BLAST [48,49] search, and the A chains of three structures of SqrE and SqrA enzymes of *A. ambivalens* and *A. aeolicus*, respectively, were selected for model building (3H8L, 3HYW and 3HYV). The BLAST similarity for these structures gave identity values of 41.4, 39.8 and 39.5, respectively. The use of multiple templates for homology modelling was necessary, as a protein complex with high similarity and containing both ligands (FAD and dUQ) was not available in the PDB database. The initial model was based on the 3H8L, and the structure of the missing C-terminal part was predicted with the help of 3HYV. Modelling the position of dUQ required the use of 3HYW template. In Prime, energy-based homology building was selected, which resulted in a single homology model. Loop refinement was also performed where unrealistic close contacts were provided. Although the model was energy-minimized during the homology building, the resulting structure was minimized once again by the Macromodel [50] module using OPLS2005 force field with implicit solvent providing a proper covalent bond structure between Cys121 amino acid and the FAD cofactor.

The model with the persulfide bond connection was derived from the single sulfur connected model. The second sulfur atom was considered as it might be present at a distance suitable for disulfide bond formation. We thus positioned the S atom of this cysteine according to this requirement. This starting position was minimized again with the Macromodel [50] package.

3. Results

3.1. Sequence comparison and structural homology model of TrSqrF

According to the classification of Marcia et al. [12], the *T. roseopersicina* TrSqrF protein belongs to the type VI SQRs [16]. We aimed to disclose the catalytic mechanism of this type VI representative enzyme. To identify residues that participate in the catalytic process, a deep interrogation of sequence databases was performed. Residues of particular interest are cysteines due to their participation in the catalytic mechanism of SQRs of other types. The TrSqrF has four cysteines in the primary sequence (Fig. 1). Cys332 is ubiquitous, while Cys 121 is identified in type I, IV, V and VI SQRs and they correspond to the highly conserved Cys347 and Cys124 of *A. aeolicus* SQR, respectively. However, there is no matching residue to the Cys156 of *A. aeolicus* enzyme in the *T. roseopersicina* and all other type VI SQR proteins. The Cys272 is a unique, characteristic conserved cysteine of the type VI SQRs. Based on the available SQR structures, the corresponding amino acids of this cysteine in type I and type V SQR proteins are localized in a surface loop
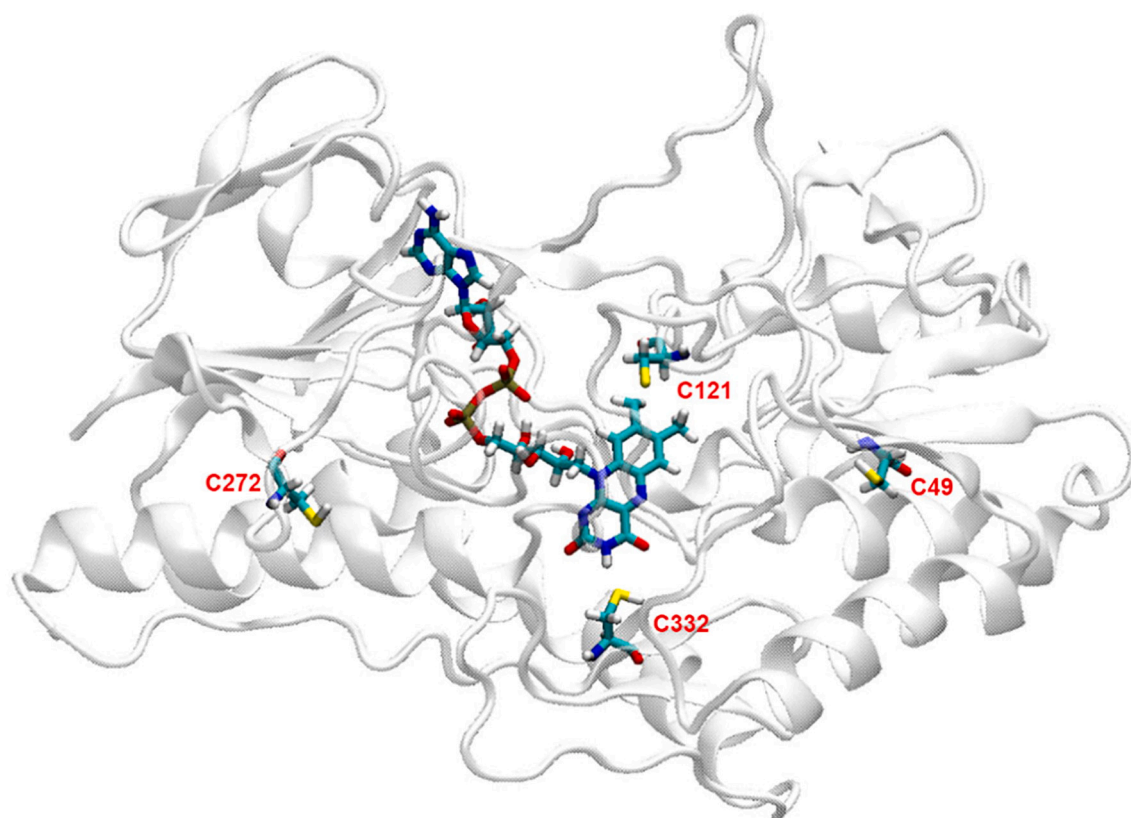
Fig. 2. The predicted position of cysteines in the homology model of *T. roseopersicina* SqrF protein. The protein backbone atoms are shown in cartoon ribbon format (white/grey). Cys residues (labelled) and FAD cofactor are shown in stick representation, coloured by atom type (C are green, O red, N blue, H white, S yellow and P brown).

[24–26]. The TrSqrF also contains a cysteine residue (Cys49) which is not conserved within any SQR type (Fig. 1).

In the absence of a crystal structure for TrSqrF, which would support a mechanistic study of the enzyme, a homology model was built for this type of SQR enzyme. Details of the computations are presented in the Materials and Methods section. The primary sequence of TrSqrF [16], its FAD cofactor as well as decylubiquinone (dUQ) ligands were also incorporated in the model building where dUQ was taken in its keto form. The conserved cysteine, Cys121 (Cys 124 in *A. aeolicus* numbering) is an obvious candidate for participation in catalysis, since its homologues residue present in other SQRs except for type II, type III and some members of type V SQR enzymes. In the case of few SQRs, this residue has been shown as an essential amino acid forming a covalent or non-covalent association with FAD and/or with one of the other conserved cysteines in the active centre [24,25]. The nature of covalent linkage to the FAD is still subject to debate in the literature. In our modelling, we considered the interaction as a permanent covalent bond [16]. The possibility of a persulfide linkage to FAD was also investigated (Fig. S1). Based on the energy-minimized structural model of TrSqrF, we analyzed the model for mechanistic possibilities with regards to reduction of FAD and its re-oxidation upon final electron transfer to dUQ. The distances of the Cys residues in the TrSqrF model were found as follows: Cys121-Cys332: 13.08 Å; Cys121-Cys49: 15.37 Å; Cys332-Cys49: 18.39 Å; Cys121-Cys272: 21.99 Å and Cys332-Cys272: 18.5 Å. These long distances raise the possibility that there is no a cysteine pair close enough to each other to form a direct disulfide bond, apparently excluding formation of such a bridge during catalysis by this enzyme (Fig. 2). So, according to our computational model, Cys121 can be positioned in the catalytic centre, with close contact between its sulf-hydryl group and the C8 methyl group of FAD (1.82 Å). Cys332 could also be found fare away (5.81 Å) from the C4 atom of the FAD

isoalloxazine ring. The third conserved cysteine, Cys272, a putative candidate to fulfil the role of the missing conserved Cys156 (*A. aeolicus* numbering), is far from the catalytic centre in our model. It is located within a flexible loop, and its thiol group is on the protein surface. The non-conserved Cys49 is also positioned close to the TrSqrF surface (Fig. 2). Considering the limitations of homology building, and regardless of their position in the structural model, all four cysteines in TrSqrF were selected for further biochemical investigation of their potential roles in the catalytic mechanism of type VI SQR enzymes.

3.2. Expression and purification of single cysteine mutant TrSqrF variants

Site-directed mutagenesis was applied for determining the role of each cysteine of TrSqrF in the catalytic mechanism. Single cysteine-to-alanine mutants were generated by quick change mutagenesis.

The TrSqrF mutants were expressed by *crtD* promoter-driven expression vectors [51] previously utilized for the production of the wild type enzyme [16]. The TrSqrF variants were expressed in *sqrD*, *sqrF* and *fccAB* triple deletion mutant *T. roseopersicina* (FOQRON) strain lacking the wild type sulfide:quinone oxidoreductases and flavocytochrome c. Based on western-blot analysis using Strep-tag II specific antibody, the expressed TrSqrF mutants were in the membrane fraction (data not shown) and produced at yields similar in the wild-type enzyme excepting the C121A mutant protein. After purification of membrane-bound proteins as described earlier [16], every of the TrSqrF variant appeared as single band with a molecular weight of approximately 44 kDa in SDS-PAGE analysis thus proving that the mutant proteins were purified to homogeneity (Fig. 3A).
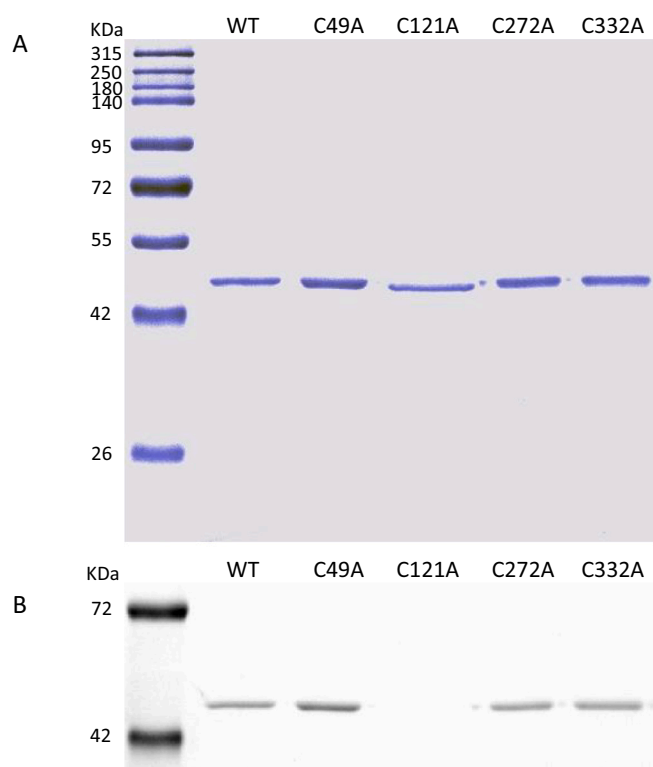
Fig. 3. Denaturing SDS-PAGE analysis of the wild type and single cysteine mutant TrSqrF protein samples expressed and purified from *T. roseopersicina*. 1 μg proteins were loaded. Standard molecular weight markers are in the first lane. A) Blue silver-stained SDS-PAGE gel. B) The same unstained SDS-PAGE gel illuminated by UV light to detect the fluorescent signal from FAD.

3.3. Spectroscopic analysis of the pure cysteine mutant TrSqrFs

Mutant proteins "as isolated" were used for recording their absorption spectra. Since the purification was performed aerobically, and even the samples were stored under air, it is feasible to suppose that the enzymes were in oxidized form. The FAD containing proteins, such as TrSqrF, can be investigated by UV–visible absorption spectroscopy. Proteins having FAD-binding sites and are in oxidized form will give two characteristic absorption peaks at 360 nm and 448 nm (Fig. 4A) [16]. However, if the reduced form of FAD is present only, no peaks will be

detected (Fig. 4A). The recorded absorption spectrum for a FAD-binding protein will give a peak profile that reflects the cumulative redox state of the FAD in the enzyme samples. Comparative analysis of the UV–Vis spectra of the wild-type and cysteine mutant TrSqrF proteins (Fig. 4B) shows that all variants, except the C121A mutant protein, contain FAD cofactor, proven by the absorption shoulder at 360 nm and a peak at 448 nm. A broad absorption band at around 675 nm has also appeared in the spectra of the wild type, C49A and C272A mutants. This indicates the presence of charge-transfer complex (CTC) between the FAD and thiolate in these proteins as reported in other SQRs [28,52] and Type II NADH:quinone oxidoreductase of *Staphylococcus aureus* [53,54], which enzymes are all members of the two-Dinucleotide Binding Domains Flavoprotein (tDBDF) superfamily. Based on the absorption spectra, FAD-protein ratios of the purified C49A, C272A and C332A TrSqrF variants were as follows: 0.85, 0.7 and 0.92, respectively. These values are similar to that of the wild type protein (0.83). In the case of the spectrum of the C121A mutant, the peak at 448 nm is missing, indicating the lack of FAD in the protein. Sequential reduction and oxidation of the C121A mutant with dithionite and then duroquinone (applied similarly as for the wild-type TrSqrF (Fig. 4A)) did not affect the absorption spectrum of this mutant. This observation further justifies that the C121A protein does not contain FAD cofactor (data not shown). FAD cofactor content was also studied with UV illumination of the SDS-PAGE gel of the purified TrSqrF variants (Fig. 3B). The fluorescent signal of FAD was not detectable in the C121A variant in contrast to the other cysteine mutant proteins, indicating that FAD binds to all mutant proteins excepting C121A variant (Fig. 3B). Differences in the absorption spectra of the purified TrSqrF mutants, focusing on the 400 nm to 500 nm wavelength range are also informative concerning the redox states of the TrSqrF variants (Fig. 4B). The absorption spectrum of the C332A sample has a profile indicating that the covalently bound FAD is oxidized in most of the protein populations. In the wild type, C49A and C272A TrSqrF mutants, a proportion of the protein contain reduced FAD (Fig. 4B). The reduction of FAD in these proteins is also supported by the presence of absorption peak characteristic of CTC. Note, that in these absorbance spectra, an additional peak at 408 nm was visible. This peak is attributed to the presence of trace amounts of cytochrome c in some samples (the extinction coefficient of the heme group at this wavelength is 170 mM^{-1} cm^{-1} [55]). The amount of c-type cytochrome is insubstantial compared with the quantity of TrSqrF in the samples. Additionally, in the SDS-PAGE gel of eluted proteins only one single band was found, verifying the purity of TrSqrF variants and the low concentration of cytochrome c content in the purified protein samples (Fig. 3A).
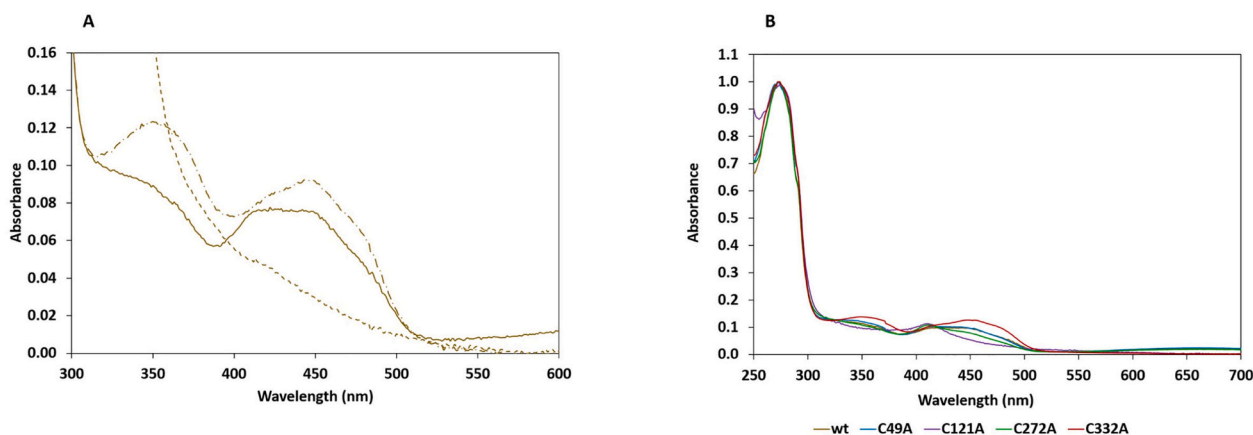

Fig. 4. UV–vis absorption spectra of the purified wild-type and mutant TrSqrF proteins. A) Spectra of the "as isolated" (solid line), dithionite (1 mM) reduced (dashed line) and duroquinone (100 μM) oxidized (dot-dashed line) TrSqrF. B) UV–vis spectra of the purified wild-type and single cysteine mutant C49A, C121A, C272A and C332A TrSqrF variants (21.5 μM, 26.3 μM, 5.2 μM, 16.3 μM and 21.8 μM, respectively), with the colour key provided. For better comparability, the absorption spectra were normalized to the same maximum absorption value.
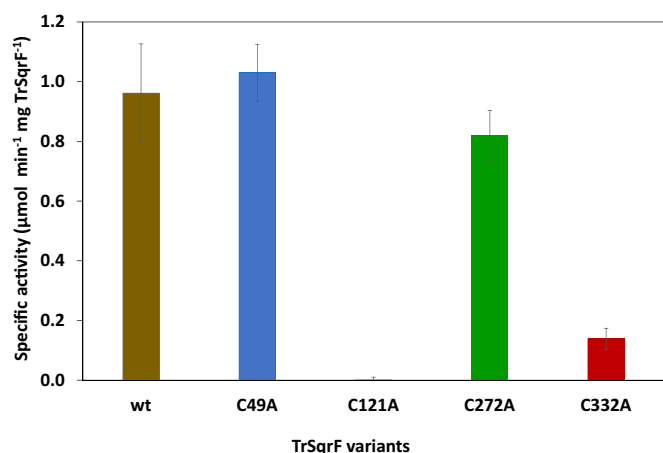
Fig. 5. Sulfide-dependent duroquinone-reducing activity of purified wild type and single cysteine mutant TrSqrF variants.

Table 1
Steady-state kinetic parameters of the wild type [16] and the cysteine mutant TrSqrF variants.

Protein	V_{max} (μmol min^{-1} mg^{-1})	k_{cat} (s^{-1})	Km (Na$_2$S) (μM)	Km (DQ) (μM)	k_{cat}/Km (Na$_2$S) (μM^{-1} s^{-1})	k_{cat}/Km (DQ) (μM^{-1} s^{-1})
SqrF wt	2.29 ± 0.19	1.64 ± 0.14	209 ± 30	27.4 ± 2.5	0.008	0.060
C49A	3.4 ± 0.1**	2.46 ± 0.07**	340 ± 8*	27.5 ± 1.8	0.007	0.089
C121A	0	0	n. d.	n. d.	n. d.	n. d.
C272A	1.4 ± 0.1**	1.01 ± 0.09**	183 ± 27	41.9 ± 3.0**	0.006	0.024
C332A	0.26 ± 0.04**	0.19 ± 0.03**	155 ± 19	35.8 ± 14.3	0.001	0.005

3.4. Enzyme activity and kinetic parameters of wild type and cysteine mutant TrSqrF variants

In our previous paper, we presented the sulfide-dependent quinone reducing activity of the wild type TrSqrF using various quinones [16]. This study indicated the ubiquinone-type compounds such as duroquinone and decylubiquinone are good substrates as final electron acceptors for this SQR. Due to its favourable solubility properties, duroquinone was chosen as the substrate for the TrSqrF variants. The sulfide-dependent duroquinone reducing activities of the cysteine mutant TrSqrF enzymes were measured at 25 °C in a standard activity assay (see Section 2.8) and compared to that of the wild type enzyme. The C49A mutant has slightly higher specific activity (1.03 ± 0.09 U mg^{-1}) than TrSqrF (0.96 ± 0.16 U mg^{-1}). The C121A variant has no activity which might be due to the lack of FAD in this enzyme. The C272A mutant has marginally reduced specific activity (0.82 ± 0.08 U mg^{-1}) while the specific activity of the C332A mutant protein is remarkably diminished (0.14 ± 0.03 U mg^{-1}) as compared to the TrSqrF enzyme activity (Fig. 5).

A steady-state kinetic study of the mutant versus wild-type enzymes can be somewhat more informative for the comparative analysis of activity, and the potential reasons for it, than specific activity measurements. The steady-state kinetic curves of cysteine mutant enzymes for sulfide and duroquinone substrates were thus measured (Fig. S3) and the data were fitted to the Michaelis-Menten equation by non-linear regression to derive the K_m, k_{cat} and k_{cat}/K_m kinetic parameters (Table 1). The C121A mutant was not active, and hence no kinetic parameters are reported for this enzyme. The C49A enzyme has slightly increased V_{max} and k_{cat} values as compared to those of wild-type TrSqrF. However, a higher K_m for sulfide, suggests that the replacement of Cys49 with alanine has caused decreased affinity for the sulfide substrate. It displays no detectable change in affinity for the dUQ substrate. The k_{cat} of the C272A variant slightly decreased, and the affinity of the C272A mutant for duroquinone (DQ) was lower (increased K_m) than those of the wild-type TrSqrF enzyme, but the mutated enzyme has a similar affinity for the sulfide substrate. Overall, this variant has a very similar specificity for sulfide to the wild type enzyme but lower specificity with the DQ substrate than wild type TrSqrF. Results with the C332A mutant TrSqrF variant are immediately more evident than the C49 and C272 mutations. The k_{cat} and the V_{max} values for the C332A variant catalyzed reaction were each one order of magnitude smaller than those data obtained with the wild type enzyme which coincided with the significantly diminished specific activity measured for this mutant enzyme (Table 1 and Fig. 5).

In the statistic analysis, significance values were calculated by Welch's t-test in R Studio software; single and double asterisks indicate p-value < 0.05 and p-value < 0.005, respectively. The p-value represents the probability that the difference between the experimental data of the mutant and the wild type enzyme could have occurred just by random chance.
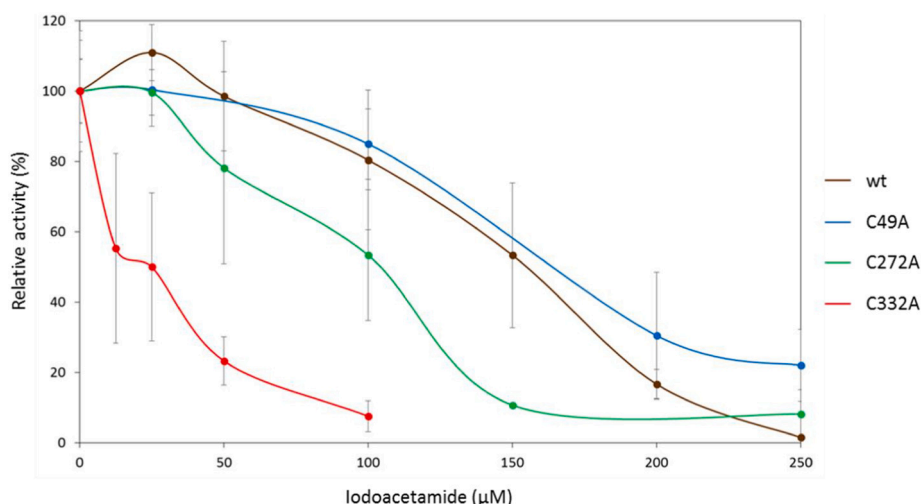

Fig. 6. The activities of the wild type and single cysteine mutant TrSqrF variants in the presence of IAA sulfhydryl reagent.
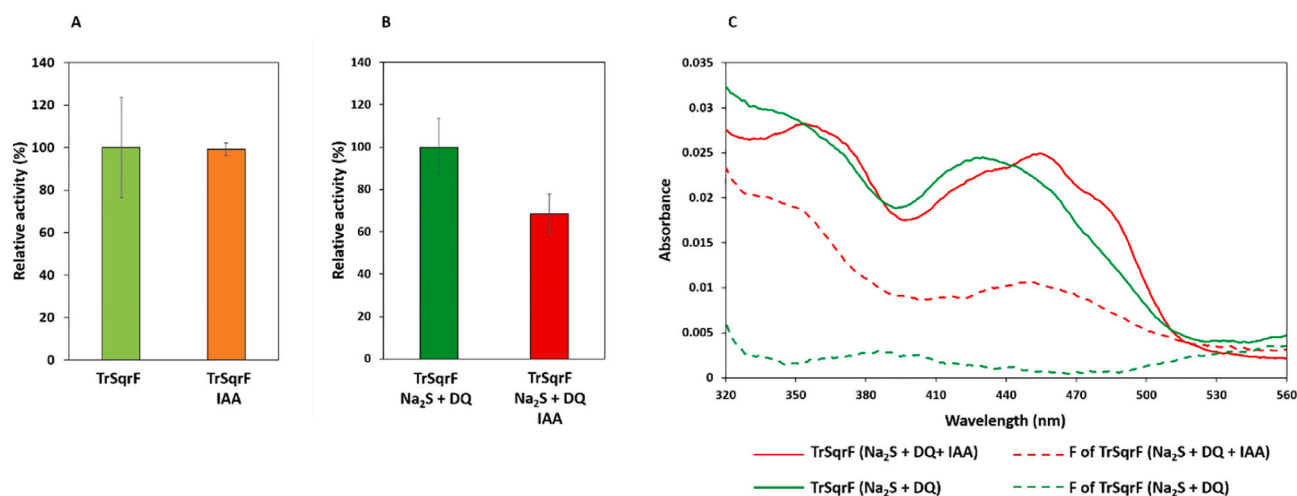
Fig. 7. Inhibition of TrSqrF by sulfhydryl blocking agent IAA. Relative activities of enzyme samples treated in the absence (A) and the presence (B) of sulfide and duroquinone substrates. (C) Absorption spectra of the samples from assays shown in panel B. Abbreviations: TrSqrF and TrSqrF (Na_2S + DQ): non-treated controls, TrSqrF IAA and TrSqrF (Na_2S + DQ + IAA) are samples pretreated by iodoacetamide in the absence and presence of the substrates, respectively. F designates the filtrate of the indicated samples (see also the text).

3.5. Inhibition of duroquinone reducing activity of wild type and cysteine mutant TrSqrF variants

To further study the role of the cysteines in the catalytic mechanism of TrSqrF, iodoacetamide (IAA) and iodoacetic acid were used as sulfhydryl blocking agents. The inhibition of TrSqrF by these reagents was followed using standard enzyme activity measurements [16]; in these cases, the sulfhydryl reagent was added to the reaction mixture containing active enzyme. IAA proved to be a better blocking agent, and the inhibition of mutant enzymes was assessed using this reagent. The duroquinone-reducing activity of the wild-type TrSqrF is completely inhibited by 300 μM IAA [16]; the IC_{50} value of the IAA reagent was 134 μM. The inhibitory effect of the reagent on the inactive C121A mutant TrSqrF was not measured. The inhibition level of the C49A mutant was similar to that of the wild type enzyme (IC_{50} = 131 μM). However, for C272A, variant was inhibited by less, 150 μM blocking agent (IC_{50} = 86 μM.). Finally, the C332A was much more sensitive to inhibition with IAA (with an IC_{50} = 15 μM) (Fig. 6). This more ready inhibition of C332A with IAA correlates with its overall decreased enzyme activity.

In the following experiments, we asked whether a resting enzyme can be blocked/inhibited by the sulfhydryl reagent. The enzymes were incubated in the presence and absence of IAA applied in higher amount (500 μM) than minimal inhibitory concentration for 10 min at 25 °C. Samples containing 3.3 μg enzymes were taken from the mixtures, and their duroquinone-reducing activities were determined using standard activity assay. It should be noted that the activity assay reaction mixture contained 1.3 μM IAA after transfer with treated enzyme sample and dilution within the assay mix. Thus, the remaining concentration of IAA in the activity assay was two orders of magnitude lower than the IC_{50} value of this agent. On comparison of activity measurements recorded using TrSqrF, and TrSqrF that has been pretreated with IAA, as above, it is important to note, that the activities were identical, suggesting that the wild type resting enzyme was not inactivated in the presence of IAA (Fig. 7A). However, the duroquinone-reducing activity of the TrSqrF protein previously preincubated with 500 μM IAA in the presence of the substrates, duroquinone (50 μM) and sulfide (200 μM), was markedly decreased to 68.5 ± 9.1%, of the normal levels, indicating that a portion of enzyme molecules was inactivated by such treatment (Fig. 7B). After the IAA treatment, UV–Vis spectra of these samples were recorded. The spectrum of the TrSqrF protein preincubated with substrates in the presence of IAA gives a slightly higher peak at 448 nm, compared to a sample without IAA, suggesting that, in the presence of IAA inhibitor, a greater proportion of the enzyme contains oxidized FAD (Fig. 7C). The inactivation effect of IAA on TrSqrF protein would appear to require the presence of substrates, and thus is only exerted on enzyme molecules that are undertaking catalysis (Fig. 7A and B).

As part of the inhibition studies, the FAD-binding to IAA-inhibited enzyme was studied. Samples of TrSqrF proteins previously treated in the presence of the substrates were precipitated with 5% trichloroacetic acid then centrifuged. The precipitated protein was collected in yellow pellets indicating the presence of FAD in these samples. The pellets were suspended and filtered (see in Section 2.9) to separate the released FAD cofactors from TrSqrF proteins. Absorption spectroscopy was then used to monitor the presence of FAD, if released from the enzyme, in the filtrate. Two absorption peaks at 360 and 448 nm indicate the presence of FAD in the filtrate for the TrSqrF protein sample preincubated with substrates and IAA (F of TrSqrF (Na_2S + DQ + IAA) in Fig. 7C but these peaks are not observed for the filtrate of the non-inhibited control protein sample (F of TrSqrF (Na_2S + DQ)). The results show that FAD is released from the enzyme in the IAA-treated sample (of which some inactivation occurs) but is not released from the non-inhibited sample, presumably remaining covalently bound in the TrSqrF enzyme (Fig. 7C). These data suggest that the covalent bond between the catalyzing enzyme and FAD got temporarily broken, allowing the binding the sulfhydryl reagent and thus releasing the cofactor.

4. Discussion

This study has focused on the catalytic function of cysteine residues in the type VI SqrF enzyme of one of the most widely studied species of purple sulfur bacteria, *Thiocapsa roseopersicina*. Despite the structural similarity, there are significant variations among the representatives of the six types of SQR enzymes in their primary sequences and kinetic properties [15,17,19,21,23,25,27,52,56–59], which likely results in possible differences in the catalytic mechanisms of various type of SQRs. Type VI SQRs are remarkably divergent, as discussed further later. Based on structural, biochemical and site-directed mutagenesis studies, a few alternative models of catalytic mechanism have been proposed for SQRs in groups outside type VI [12]. The proposed models are concordant in the essential role of conserved cysteines located in the active site in the enzymatic process. Two of the conserved cysteines form a disulfide bridge which is the redox-active centre in the catalytically active site, similarly to other members of the FDR enzyme family [14]. The models assume that cysteines in equivalent positions to the Cys156 and Cys347

residues of the *A. aeolicus* SqrA protein are candidates for the formation of the essential disulfide bond in SQRs. However, it is not possible to directly observe a disulfide bridge between these cysteines in the SQR structure. The distance between these residues is 8.31 Å and 8.8 Å in the SqrA enzymes of *A. aeolicus* and *A. ferrooxidans*, respectively [24,26], which are too long for the formation of direct disulfide bonds between these amino acids and it is proposed these cysteines are connected by polysulfur chains which are synthesized in the repeating catalytic cycles of the sulfide oxidation reaction. The equivalent residues of Cys347 are positioned in a conserved β-strand structure that forms part of the enzyme active site inside the protein [22,24–26]. However, the Cys156 (and its equivalents in homologous enzymes) is located in a loop region of the *A. aeolicus* SqrA protein [24]. Thus, the relative spatial location of the amino acid is probably flexible in the active site. At the beginning of the catalytic process, they may be located closer to each other, forming a disulfide bond which reacts with the sulfide substrate in the first reaction cycle. The third conserved cysteine is the homologue of the Cys124 of *A. aeolicus* SqrA. This residue is connected to FAD in some SQR enzymes, binding the cofactor covalently by thioether or persulfide bonds [24,25] and might also be able to form a disulfide bridge with the equivalents of the Cys156 residue during catalysis [24].

In terms of the primary and spatial structural pattern of conserved cysteines, the type VI SQRs show the most massive difference as compared to other SQR enzymes. These enzymes are typically found in bacteria that may live in environments exposed to high levels of sulfide [12,21]. Accordingly, the K_m values (for sulfide) of kinetically characterized SqrF enzymes of *C. tepidum* [21] and *T. roseopersicina* [16] are significantly higher than most other SQRs in other groups. Such differences between the type VI SQRs and other types indicate that a distinct reaction mechanism in typeVI SQR enzymes is possible. The TrSqrF protein contains four cysteines, all of which are investigated in our study; only two of these are also present in other SQR types: Cys121 and Cys332 equivalent to Cys124 and Cys 347 of *A. aeolicus* respectively (Fig. 1). Critically, an equivalent to Cys156 is not present in TrSqrF (or other members of type VI SQRs), and it would therefore appear that the proposed disulfide bridge that requires this residue in existing models of catalysis cannot form in enzymes of this group. However, type VI SQR proteins contain a conserved cysteine that is exclusive to this group (Cys272). Moreover, the TrSqrF also has a cysteine (Cys49) that is not conserved across type VI enzymes. Both these cysteines were included in our studies concerning the possible participation in catalysis. Conservation of a cysteine at the position equivalent to Cys124 would suggest that the location of this cysteine is critical to catalysis in all SQR types, regardless of the precise mechanism, presumably via interaction with FAD. Indeed, the wild type TrSqrF protein binds FAD covalently [16], similarly to SqrA of *A. aeolicus* and SqrE of *A. ambivalens* [24,25].

Our homology model of the TrSqrF protein allows us to inspect a proposed structure in the absence of a crystal structure. As expected, Cys121 and Cys332 are in the active site of the enzyme, close to the FAD cofactor (Fig. 2). In the minimized homology model, the distance between the sulfur of the side chain of Cys121 and the C8M atom of the isoalloxazine ring is 1.82 Å, which is sufficient for the formation of a covalent connection. In contrast, the Cys332 S$^\gamma$ atom was found at 5.81 Å from the C4A atom of the redox moiety of the FAD cofactor. According to the homology model, Cys272 and Cys49 residues are located near the surface of the protein, not in the active site. The distance between the cysteines of the active site (Cys121 and Cys332) was found to be too long for the formation of a disulfide bridge. Furthermore, the surface localized cysteines are also unable to connect to either of the active site cysteines because of their inter-residue distances that exceed 15 Å in every case. Therefore, the homology model confirmed our earlier proposition, based solely on primary sequence analysis, that a disulfide bridge between cysteines cannot occur in type VI SQRs. Indeed, a bioinformatic classification of SQRs excluded type VI enzymes from the sulfide:quinone oxidoreductase family, mostly due to the absence of Cys156, conserved across all other types (Fig. 1) [6]. Our homology

model supports that neither Cys272 nor Cys49 in TrSqrF can fulfil the role of the missing equivalent to Cys156. Nevertheless, biochemical characterization of two representatives of the type VI SQRs justifies that these proteins have sulfide:quinone reductase activity [16,21]. It is thus of high interest to determine how the type VI SQRs catalyze a sulfide: quinone reductase reaction.

Focusing on the roles of cysteines of type VI SQRs in the catalytic reaction mechanism, we employed site-directed mutagenesis to create and characterize single alanine mutants for each of the four cysteines. The obvious candidate cysteine in TrSqrF for forming a covalent linkage to the FAD is Cys121 (equivalent to Cys124 in *A. aeolicus*). Indeed, the change of the Cys121 residue to alanine resulted in an enzyme unable to bind FAD and loss of activity. The distance between the side chain S atom of Cys121 and the C8M group of the isoalloxazine ring is small (1.82 Å) which is suitable for the formation of a thioether bond, similar to that of the type V SQR of *A. ambivalens* [25]. It was also examined whether the structure allows accommodation of more than one sulfur atom between the FAD and the protein as seen in the structure of SqrA of *A. aeolicus* [24]. Inspection of our modelled structure found that there is enough space for inserting a second sulfur atom to form a persulfide bond (Fig. S1), as Cys121 is located within a sizeable, flexible loop region (residues 108–125) (Fig. S2), and mobility of the flexible loop could allow easy insertion of an extra atom. More precisely, the distance between the central carbon atom of the methyl group of the flavin ring and the Cα of the Cys121 changes from 3.39 Å to 3.89 Å if a second sulfur incorporates for persulfide bond formation. This spatial shift can be realizable by the long loop. Of note, though, it is worth pointing out that, although this loop naturally quite flexible, the local environment of Cys121 (Thr119 - Pro120 - Cys121 - Glu122) indicates a β-turn in this region stabilized by two structural elements. On one side, there is a weak H-bond between the backbone carboxyl group of the Thr119 and NH group of Glu122 retained whether one or two sulfurs are accommodated. On the other side, the Pro120 also promotes the formation of the turn. We propose this local β-turn structure could help direct the connection between the Cys121 and the FAD cofactor. Interestingly, this is the first report of a cysteine in this position being absolutely required for FAD binding; while the absence of FAD in C128A and C127S mutant SqrA proteins of *A. ferrooxidans* and *R. capsulatus*, respectively, was not reported [17,18].

We employed site-directed mutagenesis to create and characterize single alanine replacement mutants for each of four cysteine residues of TrSqrF. Indeed, due to the replacement of the Cys121 to Ala, the protein lost the FAD cofactor, indicating the essential role of this cysteine in cofactor binding. This experimental result clearly confirms the feasibility of our homology model, but of course, cannot exclude indubitably the possibility of an entirely differently folded protein. In the other cysteine mutants, the FAD was strongly associated with the protein. The C121A mutant TrSqrF enzyme had no sulfide-dependent quinone reductase activity, which proved that Cys121 is essential for catalysis. Furthermore, the absence of the redox cofactor in this enzyme form results in the loss of function of this mutant. The C332A mutation caused a remarkable decrease in enzyme activity but did not completely inactivate the enzyme, indicating that this residue is necessary but not essential in the catalytic process. This residual activity might be considered surprising since mutants of the equivalent Cys356 and Cys353 residues of type I SQR of *A. ferrooxidans* and *R. capsulatus* and Cys344 cysteine of type II SQR of *Staphylococcus aureus*, respectively, are entirely inactive [17,18,23]. Furthermore, the studied C332A mutation had no significant effect on the K_m of sulfide and quinone. This suggests that the conserved cysteine, participates in the catalytic process but it has no direct role in the binding and interaction with the substrates (sulfide and quinone compounds) in type VI SQRs. Notably, this might be the corresponding cysteine to Cys347 in *A. aeolicus*, which forms the disulfide active redox centre that is part of the mechanistic models for catalysis by this enzyme. The partner cysteine, as already mentioned herein, is lacking in TrSqrF (a cysteine equivalent to Cys156) and
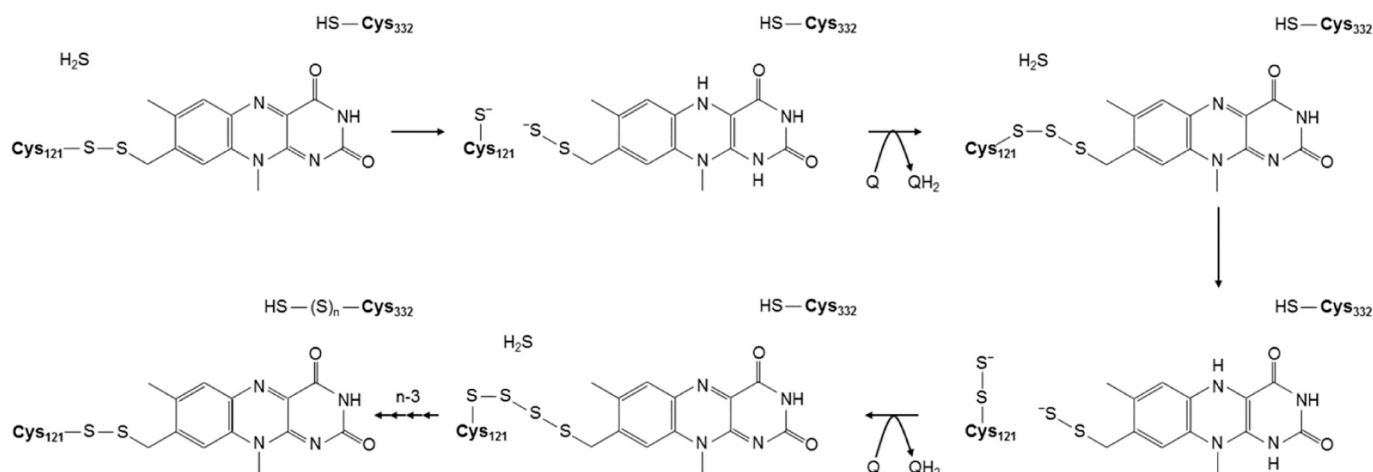
Fig. 8. A mechanistic model for catalysis of sulfide oxidation by the type VI sulfide:quinone oxidoreductase enzyme of *T. roseopersicina* based on recent biochemical analysis of wild-type and single cysteine mutant SqrF variants. In the first reaction cycle of a resting enzyme, sulfide attacks the Cys121-C8M persulfide bridge to form a Cys121 thiolate and a persulfide on the C8M methyl moiety of the isoalloxazine group of FAD as the charge transfer complex to transfer two electrons from the bound sulfide substrate to the isoalloxazine ring. The next step is the re-formation of the covalent bond between Cys121 and the cofactor, as a trisulfide bridge, and the regeneration of oxidized enzyme by reduction of the final electron acceptor quinone compound. In the following reaction cycles, each sulfide attacks the polysulfide chain bound to the cofactor connecting to the isoalloxazine ring to create the charge-transfer complex. Finally, each sulfur (oxidized sulfide) is incorporated into the polysulfide formed between the Cys121 and FAD. Cys332 may have a role in taking over the sulfur chain from the active centre of enzyme allowing to restore the sulfide non-binding enzyme form.

another type VI enzymes, uniquely in the SQR family. Hence, although involved in optimizing catalysis, Cys332 in TrSqrF cannot participate in the mechanisms as thus far proposed. All purified C332A mutants are oxidized with respect to bound FAD, suggesting that Cys332 participates in the reductive (sulfide oxidation) phase of the catalytic cycle. The demonstrated proximity of Cys332 to FAD would favour this proposal (FAD becomes reduced in this stage). The lack of the absorption peak characteristic for CTC in SQR enzymes in the spectra of C121A and C332A mutants also supports the role of these cysteines in the sulfide oxidation process.

Cys272 is a cysteine that is not present in other types of SQRs and might be a candidate for participation in catalysis in place of an equivalent residue to Cys156. Modification of Cys272 specific for the type VI SQRs slightly decreased the activity of TrSqrF and affected the K_m of duroquinone, indicating a reduced affinity for the quinone substrate. These observations confirm that Cys272 does not perform a role equivalent to the missing Cys156, but indicate that the residue, located close to the protein surface participates in the quinone reduction step of the enzyme reaction. In the TrSqrF protein, the Met156 residue is located in the analogous sequence and spatial position as Cys156 in SqrA of *A. aeolicus*. A single mutant variant of TrSqrF enzyme, in which this residue was changed to alanine, was also created. The specific activity of the M156A mutant was 1.18 ± 0.376 μmol min^{-1} mg^{-1}, which did not differ significantly from the activity of the wild-type TrSqrF, indicating that this methionine does not participate in the enzyme catalysis. Mutation of Cys49 resulted in an enzyme with equivalent, or slightly enhanced activity as compared to the wild-type TrSqrF, and with a slight reduction in affinity to sulfide. The position of this cysteine, well away from the active site, would imply that the small effects caused by its mutation are indirect and mediated, for example, by slight perturbations in protein structural stability.

The effect of the sulfhydryl-group reacting agents iodoacetamide (IAA) and iodoacetic acid on the TrSqrF enzyme was also investigated. The relative activity of TrSqrF was lower in the presence of both of these enzyme inhibitors, as observed for other SQRs [5,19,25]. However, TrSqrF enzyme samples treated with IAA in the absence of substrate molecules were not inhibited, showing that IAA can react with the active/catalyzing but not resting protein. According to our assumption, IAA blocks the catalytic process of the enzyme by reacting with cysteine

(s) for which the thiol-group is would usually be inaccessible (e.g. in a bound form) in non-catalyzing protein. To explain irreversible inhibition of a proportion of enzyme by IAA in the presence of substrates, a cysteine can move from a bound to an unbound (free) form during the catalytic process. In this state, the free sulfhydryl-group of the cysteine can react with IAA forming an irreversibly modified enzyme that cannot complete the catalytic cycle. Based on the structural model of TrSqrF, only the Cys121 can be in a covalently bound form in the protein. Moreover, the presence of FAD was detected in the supernatant of IAA-inactivated denatured enzyme samples, indicating the release of the cofactor from the inhibited enzyme. It confirms our assumption that inhibition of TrSqrF is caused by the reaction of IAA with the Cys121 residue, presumably responsible for the covalent binding of the FAD cofactor. Probably the covalent bond between the cysteine and cofactor is broken at specific points during the catalytic process allowing the reaction of IAA with the thiol-group of Cys121. In the absence of substrates, Cys121 would be covalently linked to FAD permanently, and the linkage would not be disrupted; hence, IAA does not cause irreversible enzyme inhibition. Another challenging point concerns the Cys332 residue. The C332A mutation led to dramatically reduced enzyme activity. As discussed above, this cysteine cannot be bound to other cysteines via a disulfide bridge; therefore, theoretically, it should be in thiol form. However, IAA does not block this residue in the resting enzyme indicating Cys332 in a form preventing the reaction with IAA. It is reasonable to assume that Cys332 takes over the polysulfur chain from Cys121 and thus, it cannot react with IAA.

Determination of the inhibitory concentration values of IAA for the C49A, C272A and C332A TrSqrF variants showed that the cysteine mutants, which have decreased activity relative to the wild type, could be inhibited by lower concentrations of IAA even though the protein contains fewer cysteines than the wild type enzyme. The C272A mutant is less, while the C332A variant is more sensitive to IAA dependent enzyme inhibition. These results also suggest that the thiol group of the cysteine(s) participating in the catalytic process is in a free state in part of the catalytic cycle. In single cysteine mutant TrSqrF variants showing decreased activity, especially in the C332A variant, the probability of the reaction of IAA with the free cysteine sulfhydryl-group is higher because of the time of the free-thiol, iodoacetamide reactive state of Cys121 is likely longer in a slower catalytic cycle.

According to the catalytic mechanism models of SQR enzymes, the redox-active disulfide bond between the conserved cysteines of the active site is broken by sulfide substrate. In the previously proposed mechanisms, the cysteines (Cys356, Cys156 and Cys178 in SqrA enzymes of *A. ferrooxidans*, *A. aeolicus* and SqrE of *A. ambivalens*, respectively) participates in the generation of an electron transfer transient covalent adduct with the isoalloxazine ring of FAD. The other cysteines (Cys160, Cys350 and Cys347 in *A. ferrooxidans*, *A. aeolicus* and *A. ambivalens*, respectively) will be in a free state [24–26]. Since C332A in TrSqrF is not IAA-reactive in the resting enzyme, it might not be in a free thiol state but might contain a polysulfur adduct.

Our structure-function analysis of cysteine residues in TrSqrF enabled us to construct a model for FAD cofactor binding and the mechanism of sulfide oxidation in type VI SQR enzymes to be proposed (Fig. 8). In this model, the Cys121 residue is responsible for the covalent binding of FAD by a putative persulfide-bridge between the cysteine and the C8M methyl-group of the isoalloxazine ring, similarly to the FAD-binding reported in the SqrA of *A. aeolicus* [24]. Presumably, this heterodisulfide bond is the usual redox-active centre of the type VI SQR enzyme. In the first step of the catalytic cycle, the sulfide substrate reacts with the persulfide structure and binds to the Cys121 sulfur which directly connects to the C8M moiety of the isoalloxazine ring, forming a charge-transfer complex with FAD, allowing the transfer of two electrons from the reduced sulfur to the cofactor. Due to the concomitant opening of the heterodisulfide bond, the free thiol-group of Cys121 is formed, capable of reacting with sulfhydryl-blocking reagents (such as iodoacetamide). After the oxidation of the FAD via electron transfer to a quinone molecule, Cys121 gets probably connected to the cofactor again, reforming the heterodisulfide bridge through an extended form (polysulfide) that incorporates of the oxidized sulfide into the sulfur chain. In the next catalytic cycle, a new sulfide molecule attacks the sulfur connected to the cofactor. The role of Cys332 in the catalysis of sulfide oxidation has yet to be clarified. While our kinetic data do not implicate C332A in substrate binding (which fits with our model), this conserved cysteine might participate in taking over the polysulfur chains of oxidized sulfides. This suggestion would fit with our kinetic data and inhibition study and corresponds to the proposed function of Cys347 in *A. aeolicus* SqrA [12,24].

The model, presented here, is the result of the first mechanistic study of a type VI SQR enzyme and, as such, it is both unique and unprecedented. It validates this group as bona fide SQRs, despite their exclusion in the bioinformatic classification of SQRs based on sequence conservation [6]. The model is attractive because the need for a second cysteine to form a disulfide bond, as proposed in the mechanism of other SQR types, is negated by the use of sulfur from the sulfur-rich environment of the host bacterium.

Declaration of competing interest

The authors declare that they have no known competing financial interests or personal relationships that could have appeared to influence the work reported in this paper.

Acknowledgements

Appendix A. Supplementary data

Supplementary data to this article can be found online at https://doi.org/10.1016/j.bbabio.2020.148337.

References

[1] J. Bełtowski, Hydrogen sulfide in pharmacology and medicine - an update, Pharmacol, Reports, 2015, https://doi.org/10.1016/j.pharep.2015.01.005.

[2] C. Szabo, A timeline of hydrogen sulfide (H2S) research: from environmental toxin to biological mediator, Biochem. Pharmacol. (2018), https://doi.org/10.1016/j.bcp.2017.09.010.

[3] S. Korshunov, K.R.C. Imlay, J.A. Imlay, The cytochrome bd oxidase of Escherichia coli prevents respiratory inhibition by endogenous and exogenous hydrogen sulfide, Mol. Microbiol. (2016), https://doi.org/10.1111/mmi.13372.

[4] K.R. Olson, H2S and polysulfide metabolism: conventional and unconventional pathways, Biochem. Pharmacol. (2018), https://doi.org/10.1016/j.bcp.2017.12.010.

[5] C. Griesbeck, G. Hauska, M. Schütz, Biological sulfide oxidation: sulfide-quinone reductase (SQR), the primary reaction, Recent Res. Dev. Microbiol. 4 (2000) 179–203.

[6] F.M. Sousa, J.G. Pereira, B.C. Marreiros, M.M. Pereira, Taxonomic distribution, structure/function relationship and metabolic context of the two families of sulfide dehydrogenases: SQR and FCSD, Biochim. Biophys. Acta Bioenerg. 1859 (2018) 742–753, https://doi.org/10.1016/j.bbabio.2018.04.004.

[7] R. Wang, Hydrogen sulfide: the third gasotransmitter in biology and medicine, Antioxidants Redox Signal, 2010, https://doi.org/10.1089/ars.2009.2938.

[8] L. Li, P. Rose, P.K. Moore, Hydrogen sulfide and cell signaling, Annu. Rev. Pharmacol. Toxicol. (2011), https://doi.org/10.1146/annurev-pharmtox-010510-100505.

[9] C. Szabo, Gasotransmitters in cancer: from pathophysiology to experimental therapy, Nat. Rev. Drug Discov. 15 (2016) 185–203, https://doi.org/10.1038/nrd.2015.1.

[10] H. Kimura, Hydrogen sulfide as a neuromodulator, Mol. Neurobiol. 26 (2002) 13–19, https://doi.org/10.1385/mn:26:1:013.

[11] A. Stein, S.M. Bailey, Redox biology of hydrogen sulfide: implications for physiology, pathophysiology, and pharmacology, Redox Biol. 1 (2013) 32–39, https://doi.org/10.1016/j.redox.2012.11.006.

[12] M. Marcia, U. Ermler, G. Peng, H. Michel, A new structure-based classification of sulfide:quinone oxidoreductases, Proteins Struct. Funct. Bioinforma. 78 (2010) 1073–1083, https://doi.org/10.1002/prot.22665.

[13] K.R. Olson, K.D. Straub, The role of hydrogen sulfide in evolution and the evolution of hydrogen sulfide in metabolism and signaling, Physiology. 31 (2016) 60–72, https://doi.org/10.1152/physiol.00024.2015.

[14] A. Argyrou, J.S. Blanchard, Flavoprotein disulfide reductases: advances in chemistry and function, Prog. Nucleic Acid Res. Mol. Biol. (2004), https://doi.org/10.1016/S0079-6603(04)78003-4.

[15] M. Marcia, J.D. Langer, D. Parcej, V. Vogel, G. Peng, H. Michel, Characterizing a monotopic membrane enzyme. Biochemical, enzymatic and crystallization studies on Aquifex aeolicus sulfide:quinone oxidoreductase, Biochim. Biophys. Acta - Biomembr. 1798 (2010) 2114–2123. doi:https://doi.org/10.1016/j.bbamem.2010.07.033.

[16] Á. Duzs, A. Tóth, B. Németh, T. Balogh, P.B. Kós, G. Rákhely, A novel enzyme of type VI sulfide:quinone oxidoreductases in purple sulfur photosynthetic bacteria, Appl. Microbiol. Biotechnol. 102 (2018). doi:https://doi.org/10.1007/s00253-018-8973-x.

[17] C. Griesbeck, M. Schütz, T. Schödl, S. Bathe, L. Nausch, N. Mederer, M. Vielreicher, G. Hauska, Mechanism of sulfide-quinone reductase investigated using site-directed mutagenesis and sulfur analysis, Biochemistry. 41 (2002) 11552–11565, https://doi.org/10.1021/bi026032b.

[18] M.M. Cherney, Y. Zhang, M.N.G. James, J.H. Weiner, Structure-activity characterization of sulfide:quinone oxidoreductase variants, J. Struct. Biol. 178 (2012) 319–328, https://doi.org/10.1016/j.jsb.2012.04.007.

[19] A.M. Lencina, Z. Ding, L.A. Schurig-Briccio, R.B. Gennis, Characterization of the Type III sulfide:quinone oxidoreductase from Caldivirga maquilingensis and its membrane binding, Biochim. Biophys. Acta Bioenerg. 1827 (2013) 266–275, https://doi.org/10.1016/j.bbabio.2012.10.010.

[20] J.A. Brito, T.M. Bandeiras, M. Teixeira, C. Vonrhein, M. Archer, Crystallisation and preliminary structure determination of a NADH: quinone oxidoreductase from the extremophile Acidianus ambivalens, Biochim. Biophys. Acta Proteins Proteomics. 1764 (2006) 842–845, https://doi.org/10.1016/j.bbapap.2005.09.015.

[21] K.E. Shuman, T.E. Hanson, A sulfide:quinone oxidoreductase from Chlorobaculum tepidum displays unusual kinetic properties, FEMS Microbiol. Lett. 363 (2016) 1–8, https://doi.org/10.1093/femsle/fnw100.

[22] M.R. Jackson, P.J. Loll, M.S. Jorns, X-ray structure of human sulfide:quinone oxidoreductase: insights into the mechanism of mitochondrial hydrogen sulfide oxidation, Structure. 27 (2019) 794–805.e4. doi:https://doi.org/10.1016/j.str.2019.03.002.

[23] J. Shen, H. Peng, Y. Zhang, J.C. Trinidad, D.P. Giedroc, *Staphylococcus aureus* sqr encodes a type II sulfide:quinone oxidoreductase and impacts reactive sulfur speciation in cells, Biochemistry, 2016, https://doi.org/10.1021/acs.biochem.6b00714.

[24] M. Marcia, U. Ermler, G. Peng, H. Michel, The structure of Aquifex aeolicus sulfide: quinone oxidoreductase, a basis to understand sulfide detoxification and respiration, 2009, https://doi.org/10.1073/pnas.0904165106.

[25] J.A. Brito, F.L. Sousa, M. Stelter, T.M. Bandeiras, C. Vonrhein, M. Teixeira, M. M. Pereira, M. Archer, Structural and functional insights into sulfide:quinone oxidoreductase, Biochemistry. 48 (2009) 5613–5622, https://doi.org/10.1021/bi9003827.

[26] M.M. Cherney, Y. Zhang, M. Solomonson, J.H. Weiner, M.N.G. James, Crystal structure of sulfide:quinone oxidoreductase from Acidithiobacillus ferrooxidans: insights into sulfidotrophic respiration and detoxification, J. Mol. Biol. 398 (2010) 292–305, https://doi.org/10.1016/j.jmb.2010.03.018.

[27] Y. Zhang, A. Qadri, J.H. Weiner, The quinone-binding site of Acidithiobacillus ferrooxidans sulfide:quinone oxidoreductase controls both sulfide oxidation and quinone reduction, Biochem. Cell Biol. 94 (2016) 159–166, https://doi.org/10.1139/bcb-2015-0097.

[28] T.V. Mishanina, P.K. Yadav, D.P. Ballou, R. Banerjee, Transient kinetic analysis of hydrogen sulfide oxidation catalyzed by human sulfide quinone oxidoreductase, J. Biol. Chem. (2015), https://doi.org/10.1074/jbc.M115.682369.

[29] L. V Bogorov, The properties of Thiocapsa roseopersicina, strain BBS, isolated from an estuary of the White Sea, Mikrobiologiia. 43 (1974) 326–32. http://www.ncbi.nlm.nih.gov/pubmed/4275197 (accessed January 27, 2020).

[30] G. Rakhely, A. Colbeau, J. Garin, P.M. Vignais, K.L. Kovacs, Unusual organization of the genes coding for HydSL, the stable [NiFe]hydrogenase in the photosynthetic bacterium Thiocapsa roseopersicina BBS, J. Bacteriol. 180 (1998) 1460–1465.

[31] L.S. Palágyi-Mészáros, J. Maróti, D. Latinovics, T. Balogh, É. Klement, K. F. Medzihradszky, G. Rákhely, K.L. Kovács, Electron-transfer subunits of the NiFe hydrogenases in Thiocapsa roseopersicina BBS, FEBS J. 276 (2009) 164–174, https://doi.org/10.1111/j.1742-4658.2008.06770.x.

[32] R. Tengölcs, L. Mészáros, E. Győri, Z. Doffkay, K.L. Kovács, G. Rákhely, R. Tengölics, L. Mészáros, E. Gyori, Z. Doffkay, K.L. Kovács, G. Rákhely, Connection between the membrane electron transport system and Hyn hydrogenase in the purple sulfur bacterium, Thiocapsa roseopersicina BBS, Biochim. Biophys. Acta Bioenerg. 1837 (2014) 1691–1698, https://doi.org/10.1016/j.bbabio.2014.07.021.

[33] L. Palágyi-Mészáros, The Thiocapsa roseopersicina genome project and the use of results in the hydrogenase research, Acta Biol. Szeged. 50 (2006) 169. http://www2.sci.u-szeged.hu/ABS/2006/Acta HPb/50169.pdf.

[34] M. Herrero, V. De Lorenzo, K.N. Timmis, Transposon vectors containing non-antibiotic resistance selection markers for cloning and stable chromosomal insertion of foreign genes in gram-negative bacteria, J. Bacteriol. 172 (1990) 6557–6567, https://doi.org/10.1128/jb.172.11.6557-6567.1990.

[35] N.T. Keen, S. Tamaki, D. Kobayashi, D. Trollinger, Improved broad-host-range plasmids for DNA cloning in Gram-negative bacteria, Gene, 1988, https://doi.org/10.1016/0378-1119(88)90117-5.

[36] A. Schäfer, A. Tauch, W. Jäger, J. Kalinowski, G. Thierbach, A. Pühler, Small mobilizable multi-purpose cloning vectors derived from the Escherichia coli plasmids pK18 and pK19: selection of defined deletions in the chromosome of Corynebacterium glutamicum, Gene. 145 (1994) 69–73, https://doi.org/10.1016/0378-1119(94)90324-7.

[37] N. Pfennig, Eine vollsynthetische Nährlösung zur selektiven Anreicherung einiger Schwefelpurpurbakter, Naturwissenschaften. 48 (1961) 136.

[38] B. Fodor, G. Rákhely, Á.T. Kovács, K.L. Kovács, K. At, K.L. Kovacs, Transposon mutagenesis in purple sulfur photosynthetic bacteria: identification of hypF, encoding a protein capable of processing [NiFe] hydrogenases in α, β, and γ subdivisions of the Proteobacteria, Appl. Environ. Microbiol. 67 (2001) 2476–2483, https://doi.org/10.1128/AEM.67.6.2476-2483.2001.

[39] I. Wittig, H. Schägger, Advantages and limitations of clear-native PAGE, Proteomics, 2005, https://doi.org/10.1002/pmic.200500081.

[40] G. Candiano, M. Bruschi, L. Musante, L. Santucci, G.M. Ghiggeri, B. Carnemolla, P. Orecchia, L. Zardi, P.G. Righetti, Blue silver: a very sensitive colloidal Coomassie G-250 staining for proteome analysis, Electrophoresis. 25 (2004) 1327–1333, https://doi.org/10.1002/elps.200305844.

[41] O.H. Lowry, N.J. Rosebrough, A.L. Farr, R.J. Randall, Protein measurement with the Folin phenol reagent, J. Biol. Chem. 193 (1951) 265–275.

[42] M. Degli Esposti, G. Lenaz, G. Izzo, S. Papa, Kinetics and sidedness of ubiquinol-cytochrome c reductase in beef-heart mitochondria, FEBS Lett, 1982, https://doi.org/10.1016/0014-5793(82)80713-8.

[43] R. Dorf, R. Bishop, Modern Control Systems, 11th ed., Prentice Hall, New Jersey, USA, 2011 https://doi.org/10.1109/TSMC.1981.4308749.

[44] T.B. Stanton, N.S. Jensen, Purification and characterization of NADH oxidase from Serpulina (Treponema) hyodysenteriae, J. Bacteriol. 175 (1993) 2980–2987, https://doi.org/10.1128/jb.175.10.2980-2987.1993.

[45] M.P. Jacobson, R.A. Friesner, Z. Xiang, B. Honig, On the role of the crystal environment in determining protein side-chain conformations, J. Mol. Biol. 320 (2002) 597–608, https://doi.org/10.1016/S0022-2836(02)00470-9.

[46] M.P. Jacobson, D.L. Pincus, C.S. Rapp, T.J.F. Day, B. Honig, D.E. Shaw, R. A. Friesner, A hierarchical approach to all-atom protein loop prediction, Proteins Struct. Funct. Genet. 55 (2004) 351–367, https://doi.org/10.1002/prot.10613.

[47] Schrödinger Program Suit, (2019).

[48] S.F. Altschul, W. Gish, W. Miller, E.W. Myers, D.J. Lipman, Basic local alignment search tool, J. Mol. Biol. 215 (1990) 403–410, https://doi.org/10.1016/S0022-2836(05)80360-2.

[49] T.L. Madden, R.L. Tatusov, J. Zhang, Applications of network BLAST server, Methods Enzymol. 266 (1996) 131–137, https://doi.org/10.1016/s0076-6879(96)66011-x.

[50] Schrödinger, MacroModel, 2019.

[51] B.D. Fodor, Á.T. Kovács, R. Csáki, É. Hunyadi-Gulyás, É. Klement, G. Maróti, L.S. Mészáros, K.F. Medzihradszky, G. Rákhely, K.L. Kovács, A.T. Kovács, R. Csáki, E. Hunyadi-Gulyás, E. Klement, G. Maróti, L.S. Mészáros, K.F. Medzihradszky, G. Rákhely, K.L. Kovács, Á.T. Kovács, R. Csáki, É. Hunyadi-Gulyás, É. Klement, G. Maróti, L.S. Mészáros, K.F. Medzihradszky, G. Rákhely, K.L. Kovács, A.T. Kovács, R. Csáki, E. Hunyadi-Gulyás, E. Klement, G. Maróti, L.S. Mészáros, K.F. Medzihradszky, G. Rákhely, K.L. Kovács, Modular broad-host-range expression vectors for single-protein and protein complex purification., Appl. Environ. Microbiol. 70 (2004) 712–721. doi:https://doi.org/10.1128/aem.70.2.712-721.2004.

[52] Y. Zhang, J.H. Weiner, Characterization of the kinetics and electron paramagnetic resonance spectroscopic properties of Acidithiobacillus ferrooxidans sulfide: quinone oxidoreductase (SQR), Arch. Biochem. Biophys. 564 (2014) 110–119, https://doi.org/10.1016/j.abb.2014.09.016.

[53] F.M. Sousa, F.V. Sena, A.P. Batista, D. Athayde, J.A. Brito, M. Archer, A.S. F. Oliveira, C.M. Soares, T. Catarino, M.M. Pereira, The key role of glutamate 172 in the mechanism of type II NADH:quinone oxidoreductase of Staphylococcus aureus, Biochim. Biophys. Acta Bioenerg. 1858 (2017) 823–832, https://doi.org/10.1016/j.bbabio.2017.08.002.

[54] F. V. Sena, F.M. Sousa, A.S.F. Oliveira, C.M. Soares, T. Catarino, M.M. Pereira, Regulation of the mechanism of type-II NADH:quinone oxidoreductase from S. aureus, Redox Biol. 16 (2018) 209–214. doi:https://doi.org/10.1016/j.redox.2018.02.004.

[55] O. Blum, A. Haiek, D. Cwikel, Z. Dori, T.J. Meade, H.B. Gray, Isolation of a myoglobin molten globule by selective cobalt(III)-induced unfolding, Proc. Natl. Acad. Sci. U. S. A. 95 (1998) 6659–6662, https://doi.org/10.1073/pnas.95.12.6659.

[56] J.G. Vande Weghe, D.W. Ow, A Fission Yeast Gene for Mitochondrial Sulfide Oxidation, 1999, https://doi.org/10.1074/jbc.274.19.13250.

[57] U. Theissen, W. Martin, Sulfide:quinone oxidoreductase (SQR) from the lugworm Arenicola marina shows cyanide- and thioredoxin-dependent activity, FEBS J. 275 (2008) 1131–1139, https://doi.org/10.1111/j.1742-4658.2008.06273.x.

[58] B. Arielis, Y. Shahakn, D. Taglichtsii, G. Hauska, E. Padanss, Purification and Characterization of Sulfide-Quinone Reductase, a Novel Enzyme Driving Anoxygenic Photosynthesis in Oscillatoria limnetica, 1994.

[59] M.R. Jackson, S.L. Melideo, M.S. Jorns, Human sulfide:quinone oxidoreductase catalyzes the first step in hydrogen sulfide metabolism and produces a sulfane sulfur metabolite, Biochemistry. 51 (2012) 6804–6815, https://doi.org/10.1021/bi300778t.